J Bio Tribo Corros (2017)3:17
DOI 10.1007/s40735-017-0077-0

Comparative Analysis of the Synergistic Effect of Sodium Molybdenum Oxide and Vanillin on the Corrosion Inhibition of 3CR12 Ferritic Stainless Steel and High Carbon Steel in Dilute Hydrochloric Acid

Roland Tolulope Loto[1,2]

Received: 26 January 2017 / Revised: 23 February 2017 / Accepted: 11 March 2017

Abstract Analysis of the synergistic effect of sodium molybdenum oxide and vanillin on the corrosion inhibition of high carbon steel and 3CR12 ferritic stainless steel in 2M HCl solution was done through coupon measurement, potentiodynamic polarization test and IR spectroscopy. Results show the admixture compound inhibited the corrosion of both steels, but performed more effectively on 3CR12 ferritic steel with average inhibition efficiency above 90% while the average inhibition efficiency of the compound on carbon steel was around 75%. Polarization studies showed mixed inhibiting properties of the compound on the carbon steel and anodic corrosion inhibition on the ferritic steel. The compound adsorbed over the entire carbon steel surface, but selectively precipitates at anodic sites on the stainless steel surface due to the passivation characteristics of the steel. Chemisorption mechanism was determined from thermodynamic calculations to be the mode of inhibition on the steels through the Langmuir adsorption isotherm. Infrared spectroscopy exposed the presence of the functional groups and bonds such as alcohols, phenols, primary and secondary amines and amides within the compound responsible for corrosion inhibition.

Keywords Adsorption · Corrosion · Steel · Inhibitor · Hydrochloric

✉ Roland Tolulope Loto
tolu.loto@gmail.com

[1] Department of Mechanical Engineering, Covenant University, Ota, Ogun State, Nigeria

[2] Department of Chemical, Metallurgical and Materials Engineering, Tshwane University of Technology, Pretoria, South Africa

1 Introduction

Corrosion problems are responsible for a significant percentage of the total costs for most industries every year worldwide. These problems are associated with operational setbacks, plant shutdowns and equipment maintenance, leading to recurrent partial and even total process shutdown, etc. causing in enormous economic losses [1]. However, some of the most prevalent consequences of corrosion are the loss of reliability and efficiency in manufacturing processes, industrial shutdown and failure and inline and end product contamination. Corrosion is the degradation and breakdown of a metal and its alloys due to chemical and electrochemical reactions with its environment.

Carbon steels are the largest prevalent group of alloys in engineering applications representing approximately 85% of the annual steel production worldwide; as a result, the corrosion of carbon steels is a problem of enormous practical importance. Their limited alloy content does not produce any significance in their corrosion behavior. High carbon steel contains up to about 1.5% of carbon. The presence of the extra carbon makes high carbon steel very hard. High carbon steel is used for applications in which high strength, hardness and wear resistance are necessary in marine applications, nuclear power and fossil fuel power plants, transportation, chemical processing, petroleum production and refining, pipelines, mining, construction and metal processing equipment [2]. 3CR12 stainless steel is a low-cost chromium, containing ferritic stainless steel fabricated by modifying the properties of grade 409 steel. It was developed as an alternative material of construction where the mechanical properties, corrosion resistance and fabrication requirements of other materials such as mild steel, galvanized steel, aluminum and pre-painted steels are

Published online: 22 March 2017

less satisfactory. It is resistant to mild corrosion and wet abrasion.

These metallic alloys are continuously exposed to the action of acids in a variety of ways. Acids solutions such as hydrochloric acids are extensively used in different industrial processes such as pickling, cleaning, descaling, acidizing, chemical processing and containers. The aggressive nature of these acids results in accelerated deterioration of the steels in contact with them. Appropriate corrosion control can help prevent or significantly reduce the corrosion effect on the steels such as the use of inhibitors. Corrosion inhibitors are one of the major techniques employed to stifle the rate of steel corrosion. The corrosion inhibition of metals in acidic media by different types of organic and inorganic compounds has been widely studied [3–8]. Sodium molybdenum oxide and vanillin have been used as corrosion inhibitors individually in previous research and have been proved to be effective [9–12]. Sodium molybdenum oxide can be a very effective inhibitor when combined with other chemicals [13, 14]. This research aims to study and compare the synergistic effect of sodium molybdenum oxide and vanillin on 3CR12 ferritic stainless steel and high carbon steel in hydrochloric acid.

2 Materials and Methods

2.1 Inhibiting Compound and Acid Test Solution

Equal fractions in solid white precipitates of sodium molybdenum oxide and vanillin (SMV), sourced in synthesized form from BOC Sciences, USA, are the inhibitor used for the research. Their properties are shown in Table 1. SMV was prepared in molar concentrations of 6.982×10^{-6}, 1.396×10^{-5}, 2.095×10^{-5}, 2.793×10^{-5}, 3.491×10^{-5} and 4.189×10^{-5}, respectively, per 200 mL each of 2M HCl solution. 2M HCl acid solutions was prepared by dilution of an analytical grade of H_2SO_4 acid (98%) with distilled water and used as the corrosive test environment.

2.2 Identification and Preparation of Steel Samples

Ferritic stainless steel (FSS) and high carbon steel (HCS) analyzed at the Materials Characterization Laboratory, Department of Mechanical Engineering, Covenant University, Ota, Ogun State, Nigeria, gave an average nominal percentage (%) composition as shown in Table 2. Their mechanical properties are shown in Table 3. FSS and HCS have cylindrical diameters of 1.7 and 0.7 cm with an average length of 0.7 cm, respectively.

Both steels samples were sectioned into seven (7) test samples with a median length of 0.7 mm and metallographically prepared with silicon carbide abrasive papers of 80, 200, 300 and 1000 grits before being polished with 6 μm diamond liquid, rinsed with distilled water and acetone, dried and stored in a dessicator for weight loss measurement and potentiodynamic polarization test according to ASTM G1-03(2011) [15].

2.3 Coupon Analysis

FSS and HCS steel samples were weighed and separately immersed in 200 mL of HCl solution at specific SMV concentrations for 240 h at ambient temperature of 25 °C. Each sample was removed from the solution every 24-h interval, rinsed with distilled water and acetone, dried and re-weighed according to ASTM G31-72(2004) [16]. Plots of corrosion rate, γ (mm/year) and percentage inhibition efficiency (η) versus exposure time T were plotted from the data obtained during the exposure hours. The corrosion rate (γ) is expressed as [17]:

$$\gamma = \left[\frac{87.6\omega}{DAT}\right] \quad (1)$$

where ω is the weight loss in mg, D is the density of the steel sample in g/cm^3, A is the total sample area in cm^2 and 87.6 is a constant. Inhibition efficiency (η) was determined from the relationship:

$$\eta = \left[\frac{\omega_1 - \omega_2}{\omega_1}\right] \times 100 \quad (2)$$

where ω_1 and ω_2 are the weight loss with and without specific concentrations of SMV. η was calculated at all SMV concentrations studied. Surface coverage was calculated from the formula below [18, 19]:

$$\theta = \left[1 - \frac{\omega_2}{\omega_1}\right] \quad (3)$$

where θ is the amount of SMV compound, adsorbed per gram of the steel samples. ω_1 and ω_2 are the weight loss of the steel sample with and without specific concentrations of SMV in the HCl solutions.

Table 1 Properties of the SMV-inhibiting compound

Inhibiting compound	Molecular formula	Molar mass (g mol^{-1})
Sodium molybdenum oxide	Na_2MoO_4	241.95
2-Methoxy-4-formylphenol	$C_8H_8O_3$	152.15

Table 2 Percentage nominal composition of ferritic stainless steel and high carbon steel

Ferritic stainless steel									
Element	C	Si	Mn	P	S	Cu	Ni	Cr	Fe
Composition	0.05	0.182	1.83	0.12	0.017	0.102	1.3	13	82.8
High carbon steel									
Element	C	Sb	Mn	Mo	Ni	Fe	–	–	–
Composition	2.4	0.04	0.69	0.08	0.01	96.96	–	–	–

Table 3 Mechanical properties of ferritic stainless steel and high carbon steel

Mechanical property	Ferritic stainless steel	High carbon steel
Hardness, Rockwell (HR Max)	HR C20	163
Hardness, Brinell (HB Max)	220	84
Tensile strength (Mpa)	455	540
Tensile strength, Yield (Mpa)	275	415
Elongation at break (% in 50 mm Min)	18	10
Charpy impact (J/cm^2 Min)	33.9	21

2.4 Potentiodynamic Polarization Technique

Potentiodynamic polarization test was performed with cylindrical steel electrodes of FSS and HCS embedded in resin mounts with an exposed surface area of 227 and 154 mm^2. The steel electrodes were prepared according to ASTM G59-97(2014) [20]. Test was performed at 25 °C ambient temperature with Digi-Ivy 2300 potentiostat and electrode cell containing 200 mL of the acid media, with and without SMV compound. Platinum was used as the counter electrode, and silver chloride electrode (Ag/AgCl) was the reference electrode. Potentiodynamic measurement was performed from −1.5 to +1.5 V at a scan rate of 0.002 V/s according to ASTM G102-89(2015) [21]. The corrosion current density (j_{corr}) and corrosion potential (E_{corr}) were calculated from the Tafel plots of potential versus log current. The corrosion rate (γ) and the percentage inhibition efficiency (η_2) were determined from Eq. 4.

$$\gamma = \frac{0.00327 \times J_{corr} \times E_q}{D} \quad (4)$$

where j_{corr} is the current density in μA/cm^2; D is the density in g/cm^3; E_q is the specimen equivalent weight in grams. 0.00327 is a constant for corrosion rate calculation in mm/year [22, 23]. The percentage inhibition efficiency (η_2) was calculated from corrosion rate values using the equation below:

$$\eta_2 = 1 - \left[\frac{\gamma_2}{\gamma_1}\right] \times 100 \quad (5)$$

where γ_1 and γ_2 are the corrosion rates with and without SMV inhibitor, respectively.

2.5 Infrared Spectroscopy

The SMV/acid solution before and after the weight loss test was exposed to a range of infrared ray beams from Bruker Vertex 70/70v spectrometer. The transmittance and reflectance of the infrared rays at different frequencies were translated into an IR absorption plot consisting of spectra peaks. The spectral pattern was analyzed and matched according to IR absorption table to identify the functional group contained in the compound.

3 Results and Discussion

3.1 Potentiodynamic Polarization Studies

Potentiodynamic polarization plots were obtained for HCS and FSS in 2M HCl solutions at various SMV concentrations ranging from 0 to 1.5% (0–4.19 × 10^{5}M SMV) as

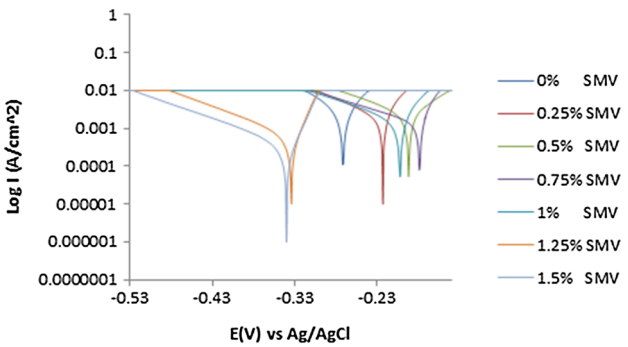

Fig. 1 Polarization plots for FSS in 2M H_2SO_4 at 0–1.5% SMV

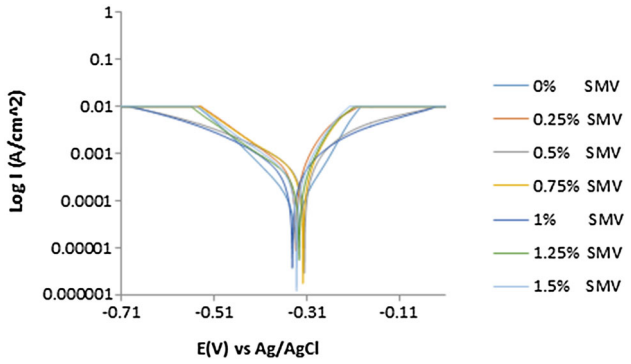

Fig. 2 Polarization plots for HCS in 2M H_2SO_4 at 0–1.5% SMV

shown in Figs. 1 and 2. Tables 4 and 5 show the results obtained from the electrochemical technique. Observation of the tables shows the remarkable difference in corrosion rate values between the uninhibited and inhibited (0.5–1.5% SMV) HCS and FSS samples due to the formation of porous oxide (rust) on the steel surface from visual observation. The redox electrochemical process and the presence of corrosive ions within the acid solution accelerate the corrosion rate according to the following equations:

The anodic dissolution mechanism of metallic alloys is:

$$Fe + Cl^- \rightarrow (FeCl^-)_{ads} \quad (6)$$

$$(FeCl^-)_{ads} \rightarrow (FeCl)_{ads} + e^- \quad (7)$$

$$(FeCl)_{ads} \rightarrow (FeCl^+)_{ads} + e^- \quad (8)$$

The cathodic hydrogen evolution mechanism is:

$$Fe + H^+ \rightarrow (FeH^+)_{ads} \quad (9)$$

$$(FeH^+)_{ads} + e^- \rightarrow (FeH)_{ads} \quad (10)$$

$$(FeH)_{ads} + H^+ + e^- \rightarrow Fe + H_2 \quad (11)$$

The cathodic oxygen reduction mechanism involves hydrogen ions with the reaction current limited not only by the oxygen diffusion but also by the hydrogen ion diffusion toward the metal surface as follows [24]:

$$O_{2,gas} + 4H^+_{aq} + 4e^-_M \rightarrow 2H_2O \quad (12)$$

The corrosion rates of the inhibited samples significantly contrast the corrosion rate values obtained at 0% SMV and remained generally the same at all SMV concentrations showing that SMV effectively inhibits the corrosion of HCS and FSS steel in HCl acid and its inhibition efficiency is slightly independent of inhibitor concentration. The Fe^{2+}

Table 4 Polarization results for FSS in 2M H_2SO_4 at 0–1.5% SMV

FSS sample	SMV conc. (M)	SMV conc. (%)	Corrosion rate (mm/year)	Inhibition efficiency (%)	Corrosion current (A)	Corrosion current density (A/cm^2)	Corrosion potential (V)	Polarization resistance, R_p (Ω)	Cathodic potential, B_c	Anodic potential, B_a
A	0	0	28.95	0	5.91E−03	2.63E−03	−0.272	27.879	−0.503	1.26E−01
B	6.98E−06	0.25	4.83	83.33	9.86E−04	4.38E−04	−0.223	4.960	−7.055	5.00E−03
C	1.40E−05	0.5	3.99	86.20	8.16E−04	3.63E−04	−0.192	5.147	−6.738	4.00E−03
D	2.09E−05	0.75	3.87	86.63	7.90E−04	3.51E−04	−0.179	5.075	−6.596	4.00E−03
E	2.79E−05	1	3.94	86.39	8.05E−04	3.58E−04	−0.202	7.526	−7.190	6.00E−03
F	3.49E−05	1.25	3.94	86.38	8.05E−04	3.58E−04	−0.334	6.335	−8.146	5.00E−03
G	4.19E−05	1.5	3.61	87.52	7.38E−04	3.28E−04	−0.340	4.185	−7.882	3.00E−03

Table 5 Polarization results for HCS in 2M H_2SO_4 at 0–1.5% SMV

HCS sample	SMV conc. (M)	SMV conc. (%)	Corrosion rate (mm/year)	SMV inhibition efficiency (%)	Corrosion current (A)	Corrosion current density (A/cm^2)	Corrosion potential (V)	Polarization resistance, R_p (Ω)	Cathodic potential, B_c	Anodic potential, B_a
A	0	0	19.09	0	6.40E−04	1.64E−03	−0.332	6.294	−10.140	7.110
B	6.98E−06	0.25	5.52	71.10	1.85E−04	4.74E−04	−0.334	54.947	−7.030	6.293
C	1.40E−05	0.5	5.49	71.26	1.84E−04	4.72E−04	−0.315	65.482	−5.560	5.157
D	2.09E−05	0.75	3.84	79.91	1.29E−04	3.30E−04	−0.318	59.454	−5.928	5.240
E	2.79E−05	1	4.43	76.80	1.49E−04	3.81E−04	−0.341	77.057	−6.509	5.937
F	3.49E−05	1.25	3.21	83.21	1.08E−04	2.76E−04	−0.326	84.082	−6.107	5.480
G	4.19E−05	1.5	4.39	76.99	1.47E−04	3.78E−04	−0.332	52.240	−6.873	5.970

ions released into the solution ($Fe \rightarrow Fe^{+2} + 2e^{-}$) react with molybdate ions component of SMV to form Fe^{2+} molybdate complex which is further oxidized by dissolved oxygen to form an insoluble, protective ferric molybdate complex in combination with ferric oxide [25]. The molybdate strengthens the outermost hydrated iron oxide layer through hydrogen bonding to hydroxide groups on the surface resulting in a negative surface charge that inhibits the diffusion of Cl^{-} to the metal surface and Fe^{2+} from the metal.

The organic inhibitor component of SMV consists of free electron pairs on the O_2 atom (reaction center) which forms coordination covalent bonds with Fe [26]. The pi-electrons of the component possibly overlap with the vacant *d*-orbitals of the metal surface. The double bonds in the molecule allow the release of Fe *d*-electrons to the π-orbitals. The organic molecules adsorb onto the corroded metal surface through displacement of adsorbed water molecules according to the general equation [27–30].

$$\mathrm{Org(sol)} + a\mathrm{H_2O(ads)} \leftrightarrow \mathrm{Org(ads)} + a\mathrm{H_2O(sol)} \qquad (13)$$

The stability of the adsorbed organic compound films/layer on the metal surface depends on the functional groups (aldehyde, hydroxyl and ether) of the compound, possible steric factors and nature of interaction between its p-orbital and the d-orbital of iron. Electrostatic attraction between the negatively charge iron surface due to Cl^{-} adsorption and the protonated inhibitor occurs. This phenomenon results in corrosion inhibition through adsorption of the ionized molecules of the inhibitor over the entire metal surface.

Corrosion potential in Table 4 shifts to anodic potentials from 0.25 to 1% SMV, showing that the combined inhibiting admixture strongly influenced the oxidation reactions at the concentrations. At 1.25 to 1.5% SMV, the corrosion potential shift to cathodic values, influencing the hydrogen evolution and oxygen reduction reactions through selective precipitation of the SMV ions on the steel surface which renders the surface passive and protected [31, 32]. These observations are illustrated in Fig. 1 where the polarization plots show wide potential behavior probably due to the passivation characteristics of FSS in interaction with the inhibitor when withstanding the action of Cl^{-} ions responsible for surface deterioration. The passive film on FSS probably breaks down and repassivates in the presence chloride ions, in HCl solution, and the breakdown site may trigger a localized corrosion of the underlying metals before inhibition. The maximum change in corrosion potential for FSS is 93 mV in the anodic direction; thus, it is an anodic type inhibitor in HCl acid [33, 34]. The polarization plots in Fig. 2 show similar electrochemical behavior due to minimal potential shifts and the lack of passivation behavior of HCS. HCS being a carbon steel undergoes general corrosion. The inhibiting actions tend to be mixed type, simultaneously influencing the redox corrosion mechanism through surface coverage. The change in polarization resistance with respect to decrease in corrosion current density in Table 5 confirms the presence of a protective film on the HCS steel surface [35–39]. The protective film controls the anodic reaction of metal dissolution ($Fe \rightarrow Fe^{2+} + 2e^{-}$) by forming Fe^{2+}—SMV complex (as earlier mentioned) on the anodic sites of the HCS surface. The maximum change in corrosion potential for HCS is 17 mV in the anodic direction; thus, its inhibiting action is mixed type inhibitor.

3.2 Coupon Analysis

Results from coupon analysis for weight loss ($\tilde{\omega}$), corrosion rate (γ) and percentage inhibition efficiency (η) for FSS and HCS samples in HCl solution at specific concentrations of SMV are detailed in Tables 5 and 6. Figures 3a, b and 4a, b show the graphical illustrations of corrosion rate and percentage inhibition efficiency versus exposure time. Observation of Figs. 3a and 4a shows the sharp contrast in the corrosion behavior of FSS and HCS samples at 0% SMV, the FSS sample corroded significantly from the onset of the exposure hours to the end with brief alternations in corrosion rate values due to the sudden destruction of its passive film. The passive film degraded probably due to the thickness and defects in the film. The film locally deteriorated and thins down before the underlying metal begins to pit at the film breakdown site from a localized mode of film dissolution because of the adsorption of chloride ions [40–44]. The corrosion rate value of HCS sample gradually increased to the end of the exposure period. Comparison of the samples shows that passivation has limited effect on the corrosion resistance of FSS samples. Addition of SMV concentrations (0.25–1.5% SMV) to the acid solution altered the corrosion behavior of FSS and HCS with SMV performing more effectively on FSS sample compared to HCS as shown in the inhibition efficiency values in Tables 6 and 7.

The corrosion inhibition efficiency of SMV on FSS (Fig. 3b) decreased at low concentrations (0.25–0.75% SMV) from about 96.9% and 91.43 to 88.33, 84.59% and 90.84%; however, after 0.75% SMV (1–1.5% SMV) the inhibition efficiency remained generally stable till the end of the exposure hours. This shows that electrochemical behavior of SMV at low concentrations is proportional to its inhibition efficiency value and is unable to remain stable due to the availability of limited SMV cations for corrosion inhibition. Similar electrochemical corrosion inhibition behavior was observed for SMV concentrations (0.5–1.5% SMV) on HCS sample after 72 h of exposure till the end of the analysis at 240 h. The inhibition efficiency

Table 6 Result for FSS in 2M HCl at specific concentrations of SMV from coupon analysis

FSS samples	Weight Loss (g)	SMV concentration (%)	SMV concentration (molarity)	Corrosion rate (mm/year)	SMV inhibition efficiency (%)
A	8.505	0	0	0.0456	0
B	0.992	0.25	6.98E−06	0.0053	88.33
C	1.311	0.5	1.4E−05	0.0070	84.59
D	0.779	0.75	2.09E−05	0.0042	90.84
E	0.295	1	2.79E−05	0.0016	96.54
F	0.312	1.25	3.49E−05	0.0017	96.34
G	0.281	1.5	4.19E−05	0.0015	96.69

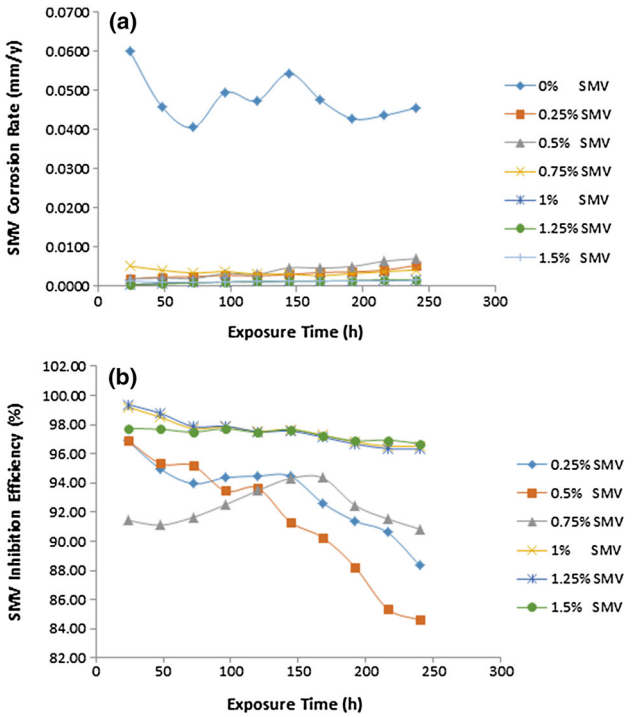

Fig. 3 Graphical illustration of **a** corrosion rate versus exposure time, **b** inhibition efficiency versus exposure time in 2M HCl at 0–1.5% SMV for FSS

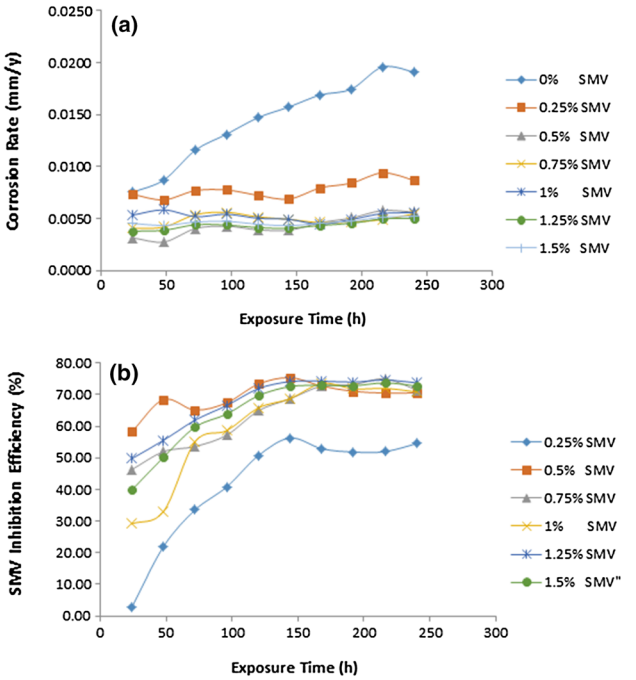

Fig. 4 Graphical illustration of **a** corrosion rate versus exposure time, **b** inhibition efficiency versus exposure time in 2M HCl at 0–1.5% SMV for HCS

increased progressively at all concentrations, confirming that total surface coverage through adsorption is the inhibition mode by SMV on HCS while selective precipitation is probably the mode of inhibition on FSS.

3.3 Adsorption Isotherm

Adsorption isotherm provides detailed insight into the physiochemical properties/interaction of the inhibitor in the acid solution at metal surface. It also shows how the adsorption process proceeds and the amount of material adsorbed for a given set of inhibitor concentration at specific temperature. The action of SMV in HCl media is assumed to be due to its adsorption at the metal/solution interface [45]. SMV blocks the metal surface and does not permit or suppresses the corrosion process from taking place. Langmuir isotherm model among others had the best fit for the results retrieved for SMV in HCl acid, respectively.

All isotherms are of the general form:

$$f(\theta, x)\exp(-a\theta) = Kc \tag{14}$$

where a is a molecular interaction parameter subject to the electrochemical interactions in the adsorption layer and the extent of inhomogeneity of the steel's surface and $f(\theta, x)$ is the configurational factor which depends on the physical model and assumptions involved in the derivation of the

Table 7 Result for HCS in 2M HCl at specific concentrations of SMV from coupon analysis

HCS samples	Weight loss (g)	SMV concentration (%)	SMV concentration (molarity)	Corrosion rate (mm/year)	SMV inhibition efficiency (%)
A	2.345	0	0	0.0191	0
B	1.066	0.25	6.98E−06	0.0087	54.55
C	0.690	0.5	1.4E−05	0.0056	70.58
D	0.671	0.75	2.09E−05	0.0055	71.40
E	0.683	1	2.79E−05	0.0056	70.89
F	0.616	1.25	3.49E−05	0.0050	73.76
G	0.639	1.5	4.19E−05	0.0052	72.76

isotherm [46, 47]. In the limit, when $x = 1$ and $a = 0$, all isotherms reduce to the Langmuir isotherm.

The general form of the Langmuir equation is shown below:

$$\left[\frac{\theta}{1-\theta}\right] = K_{\text{ads}}C \approx \theta = \theta = \left[\frac{K_{\text{ads}}C}{1+K_{ads}C}\right] \quad (15)$$

where θ is the value of surface coverage on the metal alloy, C is SMV concentration in the acid solution and K_{ads} is the equilibrium constant of the adsorption process. The plots of $\frac{C}{\theta}$ versus the SMV concentration C were linear (Fig. 5a, b) confirming Langmuir adsorption.

According to Langmuir, (1) ionized molecules of SMV selectively precipitate on adsorption sites at the metal/ion solution interface resulting in the slight deviation of the slope from unity as shown in Fig. 5a, b [48, 49], (2) the adsorption sites are equivalent and have the same binding energy to the surface and (3) the adsorption capacity is limited to one monolayer. Adsorption of SMV molecules can also be regarded as a substitution reaction in which the inhibitor molecule in the aqueous phase substitutes an x number of water molecules adsorbed on the metal surface as follows [50]:

$$I_{(\text{aq})} + x(\text{H}_2\text{O})_{\text{sur}} = I_{\text{sur}} + x(\text{H}_2\text{O})_{\text{aq}} \quad (16)$$

The quantity x has been termed the size ratio or the relative size of the SMV inhibitor to water molecules. This implies that the number of water molecules displaced depends on the size of the SMV adsorbate.

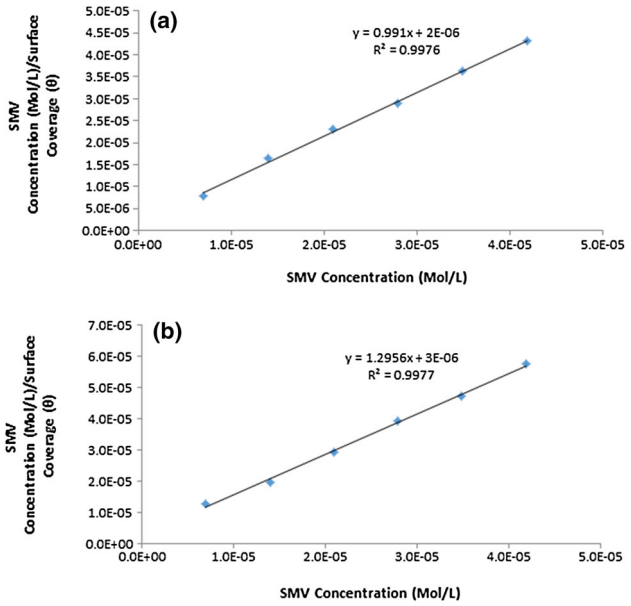

Fig. 5 Plot of $\frac{C}{\theta}$ versus SMV concentration (C) in 2M HCl **a** on FSS sample, **b** on HCS sample

3.4 Thermodynamics of the Corrosion Process

Calculated results of Gibbs free energy ($\Delta G^{o}_{\text{ads}}$) for the adsorption process as shown in Tables 8 and 9 can be evaluated from Eq. 17.

$$\Delta G_{\text{ads}} = -2.303RT\log[55.5K_{\text{ads}}] \quad (17)$$

where 55.5 is the molar concentration of water in the solution, R is the universal gas constant, T is the absolute temperature and K_{ads} is the equilibrium constant of adsorption. K_{ads} is related to the surface coverage (θ) from the relationship in Eq. 15.

The negative values of $\Delta G^{o}_{\text{ads}}$ show SMV adsorption is spontaneous. Values of $\Delta G^{o}_{\text{ads}}$ around -20 kJ mol^{-1} depict physisorption mechanism, while $\Delta G^{o}_{\text{ads}}$ around -40 kJ mol^{-1} depicts chemisorption reactions mechanisms [51]. Inhibitor chemisorption reactions form bonds with the metal surface due to charge sharing or transfer between the inhibitor cations and the valence electrons of the metal forming a coordinate covalent bond. The highest $\Delta G^{o}_{\text{ads}}$ value for FSS is -43.24 KJ mol^{-1}, while the highest for HCS is 38.67 KJ mol^{-1}. The values of $\Delta G^{o}_{\text{ads}}$ for SMV adsorption on FSS and HCS samples in HCl solution show chemisorption interaction; however, the energy of adsorption and thus the strength of inhibition are higher on FSS which confirms the results obtained from potentiodynamic polarization [52].

Table 8 Results for Gibbs free energy, surface coverage and equilibrium constant of adsorption for SMV concentrations on FSS in 2M HCl

Samples	SMV concentration (molarity)	Surface coverage (θ)	Equilibrium constant of adsorption (K)	Gibbs Free energy, ΔG (kJ mol^{-1})
A	0	0	0	0
B	6.98E−06	0.883	1,084,240.58	−44.37
C	1.40E−05	0.846	393,147.47	−41.86
D	2.10E−05	0.908	473,297.50	−42.32
E	2.79E−05	0.965	997,916.54	−44.16
F	3.49E−05	0.963	752,964.81	−43.47
G	4.19E−05	0.967	698,374.50	−43.28

Table 9 Results for Gibbs free energy, surface coverage and equilibrium constant of adsorption for SMV concentrations on HCS in 2M HCl

Samples	SMV concentration (molarity)	Surface coverage (θ)	Equilibrium constant of adsorption (K)	Gibbs Free energy, ΔG (kJ mol^{-1})
A	0	0	0	0
B	6.98E−06	0.546	171,930.0	−39.82
C	1.40E−05	0.706	171,811.3	−39.82
D	2.10E−05	0.714	119,185.9	−38.92
E	2.79E−05	0.709	87,189.1	−38.14
F	3.49E−05	0.738	80,510.2	−37.94
G	4.19E−05	0.728	63,746.5	−37.37

3.5 IR Spectroscopy

Identification and nature of the functional groups responsible for SMV inhibition on FSS and HCS in HCl solution were determined through IR spectroscopy. Figure 6 shows the superimposed spectra peaks for SMV compound on FSS in HCl before and after the corrosion test (with and without the presence of FSS sample), while Fig. 7 shows the superimposed spectra peaks for SMV-inhibiting compound on HCS in HCl solution before and after the corrosion test. The extracted table of characteristic IR absorptions is presented in Table 10. Observation of the spectra peaks in Fig. 6 shows very close similarities in the adsorption spectra, suggesting that the dominant anodic inhibition properties of SMV on FSS inhibition are through modification of the corrosive environment and selective precipitation on anodic sites on the steel. Adsorption of the functional groups of SMV would have played limited role in inhibiting the Cl^- due to the passivation characteristics of the steel and thus aid in the repassivation of the steel and corrosion inhibition through surface blockage. Matching the spectra peaks in Table 10, peak values of 3348.27 and 1635.70 cm^{-1} are revealed before corrosion test. This corresponds to the presence of alcohols, phenols, primary and secondary amines and amides functional groups. The peak values after the corrosion test were slightly similar to values before the corrosion test.

The spectra peaks in Fig. 7 showed significant difference in transmittance indicators and adsorption spectra values for SMV compound before and after the corrosion test. The functional groups of alkynes, alkyl halides, alcohols, carboxylic acids, esters, ethers, aliphatic amines and alkenes at 1220.38 and 663.95 cm^{-1} before the corrosion test completely disappeared after the corrosion test due to strong adsorption onto the HCS steel. The functional groups of phenols, primary and secondary amines and amides remained largely intact probably playing a role in modification of the corrosive environment. The adsorption of the earlier mentioned functional groups is responsible for the mixed inhibiting properties of SMV on HCS through chemisorption mechanism. SMV adsorbs over the entire surface of HCS simultaneously inhibiting the anodic and cathodic corrosion reaction processes. The groups are responsible for the formation of stable complexes between the iron constituents and functional groups present in SMV compound forming covalent or coordinate bonds between the ionic components of SMV and vacant Fe *d*-orbital.

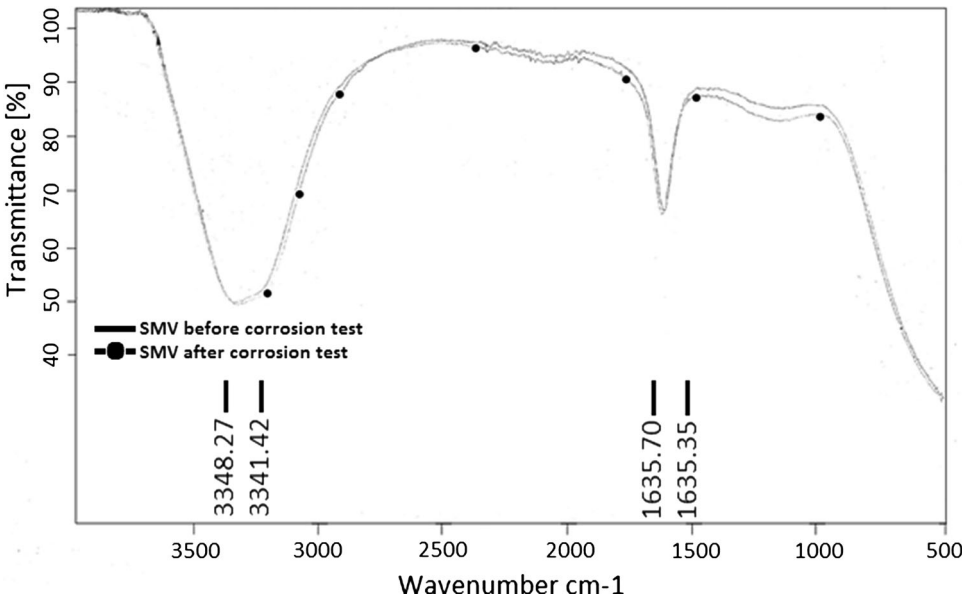

Fig. 6 IR spectra of SMV-inhibiting compound on FSS in HCl before and after corrosion test

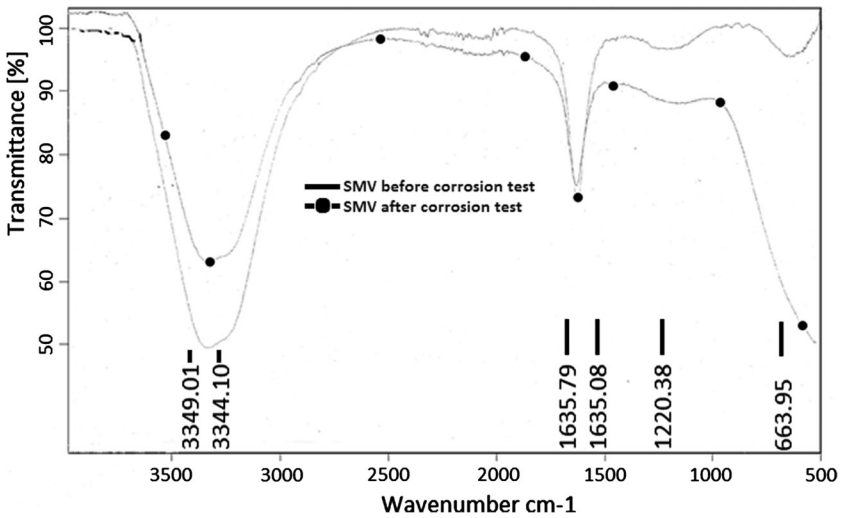

Fig. 7 IR spectra of SMV-inhibiting compound on FSS in HCl before and after corrosion test

Table 10 Table of characteristic IR absorptions

Wavenumber ($cm^{-1)}$	Bond	Functional group
3500–3200 (s, b)	O–H stretch, H–bonded	Alcohols, phenols
3400–3250 (m)	N–H stretch	Primary, secondary amines, amides
1650–1580 (m)	N–H bend	Primary amines
700–610 (b, s)	–C(triple bond)C–H: C–H bend	Alkynes
690–515 (m)	C–Br stretch	Alkyl halides
850–550 (m)	C–Cl stretch	Alkyl halides
1320–1000 (s)	C–O stretch	Alcohols, carboxylic acids, esters, ethers
1300–1150 (m)	C–H wag (–CH2X)	Alkyl halides
1300–1150 (m)	C–H wag (–CH2X)	Alkyl halides
1250–1020 (m)	C–N stretch	Aliphatic amines
1000–650 (s)	=C–H bend	Alkenes

m medium, *w* weak, *s* strong, *n* narrow, *b* broad, *sh* sharp

4 Conclusion

High carbon steel and 3CR12 ferritic stainless steel are both ferrous alloys due to their substrate iron metal composition; however, their response to corrosion under the inhibiting action of sodium molybdenum oxide and vanillin compounds in dilute HCl is quite different due to the passivation characteristics of the stainless steel. The combined admixture performed more effectively on the ferritic steel through selective precipitation on the anodic sites on the stainless steel in comparison with the mixed inhibition behavior of the compound on the carbon steel despite its hardened metallurgy and pearlite microstructure due to high carbon content. The compound inhibited corrosion through the combined action of modification of the corrosive environment and adsorption through chemisorption mechanism where the amine functional group played a major role

Acknowledgements The authors are grateful to Covenant University for the sponsorship of the research and provision of research facilities.

Compliance with ethical standards

Conflict of interest The authors declare no conflict of interest.

References

1. Garcia-Arriaga V, Alvarez-Ramirez J, Amaya Sosa ME (2010) H_2S and O_2 influence on the corrosion of carbon steel immersed in a solution containing 3M diethanolamine. Corros Sci 52(7):2268–2279. doi:10.1016/j.corsci.2010.03.016
2. Ramesh S, Rajeswari S, Maruthamuthu S (2003) Effect of inhibitors and biocide on corrosion control of mild steel in natural aqueous environment. Mater Lett 57(29):4547–4554. doi:10.1016/S0167-577X(03),00360-4
3. Jackson J, Finsgar M (2014) Application of corrosion inhibitors for steels in acidic media for the oil and gas industry: a review. Corros Sci 86:17–41. doi:10.1016/j.corsci.2014.04.044
4. Bockris JOM, Yang B (1991) Mechanism of corrosion inhibition of iron in acid solution by acetylenic alcohols. J Electrochem Soc 138:2237–2252
5. Kertit S, Elkholy A, Aride J, Srhiri A, Ben Bachir A, Etman M (1989) Chemical and electrochemical inhibition studies of corrosion and hydrogen surface embrittlement. I. $Fe_{0.78}B_{0.13}Si_{0.09}$ amorphous alloy in molar HCl. J Appl Electrochem 19(1):83–89. doi:10.1007/BF01039394
6. Edrah S, Hasan SK (2010) Studies on thiourea derivatives as corrosion inhibitor for aluminum in sodium hydroxide Solution. J Appl Sci Res 6(8):1045–1049
7. Bazzi L, Salghi R, Bouchtart A, El Alami Z, Kertit S (2002) The inhibition effect of inorganic compounds on the corrosion of the 3003 aluminium alloy in the presence of sodium chloride. Rev Met Paris 99(2):189–197. doi:10.1051/metal:2002192
8. Atmani F, Lahem D, Poelman M, Buess-Herman C, Olivier MG (2013) Mild steel corrosion in chloride environment: effect of surface preparation and influence of inorganic inhibitors. Corros Eng, Sci Technol 48(1):9–18. doi:10.1179/1743278212Y.0000000037
9. Yufei K, Fang C, Ao X (2013) Molybdate-based corrosion inhibitor system for carbon steel in sea ice melt-water. Desalin Water Treat 51(16–18):3133–3137. doi:10.1080/19443994.2012.749006
10. Lizlovs EA (1976) Molybdates as corrosion inhibitors in the presence of chlorides. Corrosion 32(7):263–266. doi:10.5006/0010-9312-32.7.263
11. Lia X, Dengb S, Fua H (2010) Adsorption and inhibition effect of vanillin on cold rolled steel in 3.0M H_3PO_4. Prog Org Coat 67(4):420–426. doi:10.1016/j.porgcoat.2009.12.006
12. Loto RT (2016) Electrochemical analysis of the corrosion inhibition properties of 4-hydroxy-3-methoxybenzaldehyde on low carbon steel in dilute acid media. Cogent Eng 3:1242107. doi:10.1080/23311916.2016.1242107
13. Pryor MJ, Cohen M (1953) The inhibition of the corrosion of iron by some anodic inhibitors. J Electrochem Soc 100(5):203–215. doi:10.1149/1.2781106
14. Emregüla KC, Hayvalıb M (2004) Studies on the effect of vanillin and protocatechualdehyde on the corrosion of steel in hydrochloric acid. Mater Chem Phys 83(2–3):209–216
15. Standard practice for preparing, cleaning, and evaluating corrosion test specimens. https://www.astm.org/Standards/G1.htm. Accessed 12 Jan 2017
16. Standard practice for laboratory immersion corrosion testing of metals. https://www.astm.org/DATABASE.CART/HISTORICAL/G31-72R04.htm. Accessed 12 Jan 2017
17. Venkatesan P, Anand B, Matheswaran P (2009) Influence of formazan derivatives on corrosion inhibition of mild steel in hydrochloric acid medium. Eur J Chem 6(S1):S438–S444. doi:10.1155/2009/507383
18. Abbasova VM, Abd El-Lateefa HM, Aliyevaa LI, Qasimova EE, Ismayilova IT, Khalaf MM (2013) A study of the corrosion inhibition of mild steel C1018 in CO_2-saturated brine using some novel surfactants based on corn oil. Egypt J Pet 4(22):451–470. doi:10.1016/j.ejpe.2013.11.002
19. Sethi T, Chaturvedi A, Mathur RK (2007) Corrosion inhibitory effects of some Schiff's bases on mild steel in acid media. J Chil Chem Soc 52(3):1206–1213. doi:10.4067/S0717-97072007000300003
20. Standard Test Method for Conducting Potentiodynamic Polarization Resistance Measurements. https://www.astm.org/Standards/G59.htm. Accessed 12 Jan 2017
21. Standard Practice for Calculation of Corrosion Rates and Related Information from Electrochemical Measurements. https://www.astm.org/Standards/G102.htm. Accessed 12 Jan 2017
22. Ahmad K (2006) Principles of corrosion engineering and corrosion control. Butterworth-Heinemann, Oxford, UK
23. Choi Y, Nesic S, Ling S (2011) Effect of H_2S on the CO_2 corrosion of carbon steel in acidic solutions. Electrochim Acta 56(4):1752–1760. doi:10.1016/j.electacta.2010.08.049
24. Okamoto G, Shibata T, Sato N (1969) Reports of Asahi glass foundation for industrial technology, vol 15. Asahi Glass Foundation for Industrial Technology, Tokyo, pp 207–230
25. Thompson SC. Molybdates: an alternative to hexavalent chromates in corrosion prevention and control. http://infohouse.p2ric.org/ref/29/28424.pdf. Accessed 14 January 2017
26. Trabanelli G, Carassiti V (1970) Advances in corrosion science and technology, vol 1. Plenum Press, New York, p 147
27. Desimonea MP, Grundmeier G, Gordilloc G, Simison SN (2011) Amphiphilic amido-amine as an effective corrosion inhibitor for mild steel exposed to CO_2 saturated solution: polarization, EIS and PM-IRRAS studies. Electrochim Acta 56(8):2990–2998. doi:10.1016/j.electacta.2011.01.009
28. Bockris JOM, Swinkels DAJ (1964) Adsorption of n-decylamine on solid metal electrodes. J Electrochem Soc 111(6):736–743. doi:10.1149/1.2426222

29. Li X, Dengb S, Fua H, Lia T (2009) Adsorption and inhibition effect of 6-benzylaminopurine on cold rolled steel in 1.0M HCl. Electrochim Acta 54(16):4089–4098. doi:10.1016/j.electacta.2009.02.084
30. Sahin M, Bilgic S, Yilmaz H (2002) The inhibition effects of some cyclic nitrogen compounds on the corrosion of the steel in NaCl mediums. Appl Surf Sci 195(1–4):1–7. doi:10.1016/S0169-4332(01),00783-8
31. Bentley AJ, Earwakera LG, Farr JPG, Saremi M, Seeney AM (1986) Molybdates in aqueous corrosion inhibition III. Effects of molybdate in the anodic filming of steel. Polyhedron 5(1–2):547–550. doi:10.1016/S0277-5387(00),84962-1
32. Sakashita M, Sato N (1977) The effect of molybdate anion on the ion-selectivity of hydrous ferric oxide films in chloride solutions. Corros Sci 17(6):473–486. doi:10.1016/0010-938X(77),90003-8
33. Susai RS, Mary R, Noreen A, Ramaraj R (2002) Synergistic corrosion inhibition by the sodium dodecylsulphate–Zn^{2+} system. Corros Sci 44(10):2243–2252. doi:10.1016/S0010-938X(02),00052-5
34. Sahin M, Bilgiç S, Yılmaz H (2002) The inhibition effects of some cyclic nitrogen compounds on the corrosion of the steel in NaCl mediums. Appl Surf Sci 195(104):1–7. doi:10.1016/S0169-4332(01),00783-8
35. Roque JM, Pandiyan T, Cruz J, Garcia-Ochoa E (2008) DFT and electrochemical studies of tris(benzimidazole-2-ylmethyl)amine as an efficient corrosion inhibitor for carbon steel surface. Corros Sci 50(3):614–624. doi:10.1016/j.corsci.2007.11.012
36. Benali O, Larabi L, Traisnel M, Gengembre L, Harek Y (2007) Electrochemical, theoretical and XPS studies of 2-mercapto-1-methylimidazole adsorption on carbon steel in 1M $HClO_4$. Appl Surf Sci 253(14):6130–6139. doi:10.1016/j.apsusc.2007.01.075
37. Kellou-Kerkouche F, Benchettara A, Amara S (2008) Effect of sodium dodecyl benzene sulfonate on the corrosion inhibition of Fe–1Ti–20C alloy in 0.5M H_2SO_4. Mater Chem Phys 110(1):26–33. doi:10.1016/j.matchemphys.2008.01.005
38. Selvi JA, Rajendran S, Ganga SV, Amalraj JA, Narayanasamy B (2009) Corrosion inhibition by beet root extract. Port Electrochim Acta 27(1):1–11
39. Rajendran S, Paulraj J, Rengan P, Jeyasundari J, Manivannan M (2013) Corrosion resistance of 18 carat gold in artificial saliva in presence of d-glucose. Eur Chem Bull 2(6):389–392
40. Fushimi K, Seo M (2001) Initiation of a local breakdown of passive film on iron due to chloride ions generated by a liquid-phase ion-gun for local breakdown. J Electrochem Soc 148(11):B450–B456. doi:10.1149/1.1407832
41. Fushimi K, Azumi K, Seo M (2000) Use of a liquid-phase ion-gun for local breakdown of the passive film on iron. J Electrochem Soc 147(2):552–557. doi:10.1149/1.1393231
42. Heusler KE, Fisher L (1976) Kinetics of pit initiation at passive iron. Mater Corros 27(8):551–556. doi:10.1002/maco.19760270802
43. Shibata T (1990) Stochastic studies of passivity breakdown. Corros Sci 31:413–423. doi:10.1016/0010-938X(90)90140-Z
44. Sato N (1976) Stochastic process of chloride-pit generation in passive stainless steel. J Electrochem Soc 123(8):1197–1199. doi:10.1149/1.2133034
45. Aramaki K, Node Y, Nishihara H (1990) Adsorption and corrosion inhibition effect of polar organic compounds on iron in 1M HClO4 containing SH−. J Electrochem Soc 137:1354–1358. doi:10.1149/1.2086673
46. Ateya B, El-Anadouli BE, El-Nizamy F (1984) The adsorption of thiourea on mild steel. Corros Sci 24(6):509–515. doi:10.1016/0010-938X(84),90033-7
47. Dhar HP, Conway BE, Joshi KM (1973) On the form of adsorption isotherms for substitutional adsorption of molecules of different sizes. Electrochim Acta 18(11):789–798. doi:10.1016/0013-4686(73),85030-3
48. Abiola OK (2006) Adsorption of 3-(4-amino-2-methyl-5-pyrimidyl methyl)-4-methyl thiazolium chloride on mild steel. Corros Sci 48(10):3078–3090. doi:10.1016/j.corsci.2005.12.001
49. Bockris JOM (1970) Modern electrochemistry, vol 2. Macdonald Ltd., London, p 772
50. Ateya B, El-Anadouli BE, El-Nizamy F (1984) The adsorption of thiourea on mild steel. Corros Sci 24(6):509–515
51. Donnely B, Downie TC, Grzeskowiak R, Hamburg HR, Short D (1978) The effect of electronic delocalization in organic groups in substituted thiocarbonyl RCSNH2 and related compounds on inhibition efficiency. Corros Sci 18(2):109–116
52. Benali O, Benmehdi H, Hasnaoui O, Selles C, Salghi R (2013) Green corrosion inhibitor: Inhibitive action of tannin extract of Chamaerops humilis plant for the corrosion of mild steel in 0.5M H_2SO_4. J Mater Environ Sci 4(1):127–138